

Proposal for a phase-coherent thermoelectric transistor

F. Giazotto,^{1, a)} J. W. A. Robinson,^{2, b)} J. S. Moodera,³ and F. S. Bergeret^{4, 5, c)}

¹⁾NEST, Istituto Nanoscienze-CNR and Scuola Normale Superiore, I-56127 Pisa, Italy

²⁾Department of Materials Science and Metallurgy, University of Cambridge, 27 Charles Babbage Road, Cambridge CB3 0FS, UK

³⁾Department of Physics and Francis Bitter Magnet Lab, Massachusetts Institute of Technology, Cambridge, Massachusetts 02139, USA

⁴⁾Centro de Física de Materiales (CFM-MPC), Centro Mixto CSIC-UPV/EHU, Manuel de Lardizabal 4, E-20018 San Sebastián, Spain

⁵⁾Donostia International Physics Center (DIPC), Manuel de Lardizabal 5, E-20018 San Sebastián, Spain

Identifying materials and devices which offer efficient thermoelectric effects at low temperature is a major obstacle for the development of thermal management strategies for low-temperature electronic systems. Superconductors cannot offer a solution since their near perfect electron-hole symmetry leads to a negligible thermoelectric response; however, here we demonstrate theoretically a superconducting thermoelectric transistor which offers unparalleled figures of merit of up to ~ 45 and Seebeck coefficients as large as a few mV/K at sub-Kelvin temperatures. The device is also phase-tunable meaning its thermoelectric response for power generation can be precisely controlled with a small magnetic field. Our concept is based on a superconductor-normal metal-superconductor interferometer in which the normal metal weak-link is tunnel coupled to a ferromagnetic insulator and a Zeeman split superconductor. Upon application of an external magnetic flux, the interferometer enables phase-coherent manipulation of thermoelectric properties whilst offering efficiencies which approach the Carnot limit.

It is known that electron-hole symmetry breaking is essential for a material to possess a finite thermoelectric figure of merit^{1,2}. In principle, conventional superconductors have a near perfect symmetric spectrum and therefore are not suitable for thermoelectric devices. However, if the density of states is spin-split by a Zeeman field a superconductor-ferromagnet hybrid device can provide a thermoelectric effect³⁻⁵ with a figure of merit close to 1. Here we propose a multifunctional phase-coherent superconducting transistor in which the thermoelectric efficiency is tunable through an externally applied magnetic flux. A giant Seebeck coefficient of several mV/K and a figure of merit close to ~ 45 is predicted for realistic materials parameters and materials combinations.

The phase-coherent thermoelectric transistor is based on two building blocks. The first one is sketched in Fig. 1(a) and consists of a superconducting film (S_R) tunnel-coupled to a normal metal (N) by a ferromagnetic insulator (FI). The latter induces an exchange field (h) in S_R which leads to a Zeeman spin-split superconducting DoS. The spectrum for spin-up (\uparrow) and spin-down (\downarrow) electrons is given by

$$v_{S_{R(\downarrow)}}(E) = \frac{1}{2} v_{BCS}(E \pm h), \quad (1)$$

where $v_{BCS}(E) = |\text{Re}[(E + i\Gamma)/\sqrt{(E + i\Gamma)^2 + \Delta_R^2(T, h)}]|$ is the conventional Bardeen-Cooper-Schrieffer DoS in a superconductor, E is the energy, Δ_R is the order parameter, and Γ accounts for broadening. Due to the presence of the spin-splitting field, Δ_R depends on temperature (T) and h . While the total DoS of S_R , $v_{S_R}(E) = v_{S_{R\uparrow}}(E) + v_{S_{R\downarrow}}(E)$, is electron-hole symmetric [Fig. 1(b)], the spin-dependent

$v_{S_{R(\downarrow)}}(E)$ components are no longer even functions of the energy. This means that electron-hole imbalance can, in principle, be achieved using a spin-filter contact with a normal metal. This would yield a finite thermoelectric effect^{3,4} in the N/FI/ S_R heterostructure shown in Fig. 1(a). In addition to providing a Zeeman splitting, the FI also serves as a spin-filter between both metals. Therefore, if one applies a temperature difference δT between N and S_R , a finite charge current (I) will flow through the junction due to the thermoelectric effect, which is given by $I = \alpha \delta T / T$. The thermoelectric coefficient α is given by⁴

$$\alpha = \frac{P}{eR_T} \int_{-\infty}^{\infty} dE \frac{E v_N(E) [v_{S_{R\uparrow}}(E) - v_{S_{R\downarrow}}(E)]}{4k_B T \cosh^2\left(\frac{E}{2k_B T}\right)}, \quad (2)$$

where P is the spin polarization due to the spin-filtering action of the FI, T is the average temperature of N and S_R , k_B is the Boltzmann constant, R_T is the junction resistance, and $v_N(E)$ is the DoS of the N layer.

Our proposal is based on the following observation: if one tunes the DoS in N in such a way that $v_N(E)$ is enhanced at those energies where the coherent peaks of the Zeeman-split superconductor occur, then α should drastically increase in accordance to Eq. (2). Ideally, one would search for a material with a tunable DoS and this can be realized with our second building block: a *proximity* superconducting quantum interference device (SQUID), as sketched in Fig. 1(c). This consists of a superconducting loop interrupted by a normal metal wire. The contacts between N and S_L are assumed to be transparent thus allowing superconducting correlations to be induced in the N region. The latter manifest as opening a gap in the N metal DoS with an amplitude that can be controlled via the quantum phase difference (φ) across the wire. Moreover, φ can be controlled via an externally applied magnetic flux Φ according to $\varphi = 2\pi\Phi/\Phi_0$, where $\Phi_0 \simeq 2 \times 10^{-15}$ Wb is the flux quantum. If the length (L) of the wire is smaller than the characteristic penetration of the superconducting cor-

^{a)}Electronic mail: giazotto@sns.it

^{b)}Electronic mail: jjr33@cam.ac.uk

^{c)}Electronic mail: sebastian.bergeret@ehu.es

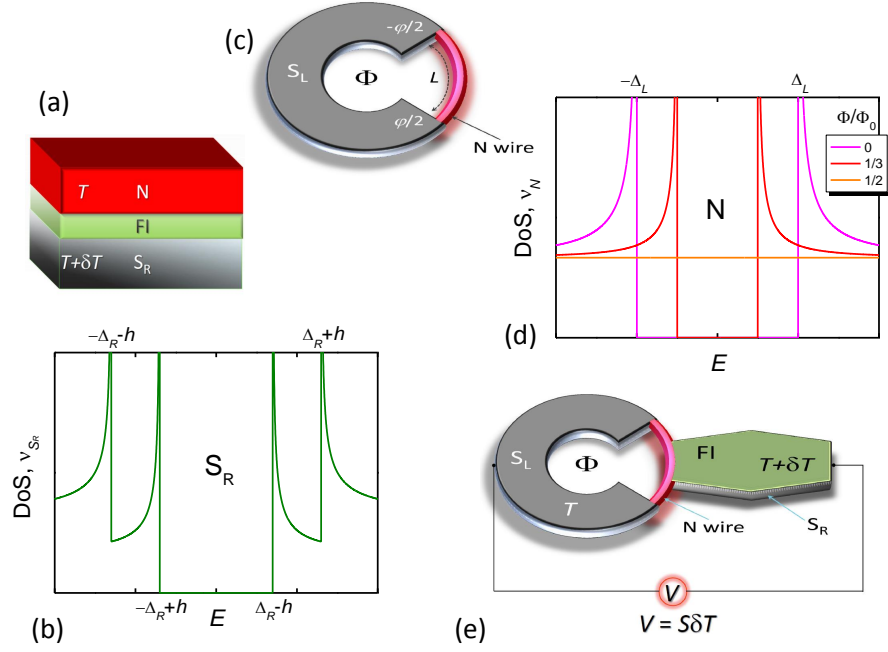


FIG. 1. The phase-coherent thermoelectric transistor. (a) Sequence of stacked metallic layers consisting of a superconductor (S_R) tunnel-coupled to a normal metal (N) through a ferromagnetic insulator (FI). This implements the thermoelectric building block of the transistor. The FI layer induces an exchange field (h) in the superconductor and simultaneously provides a spin-polarizing barrier of polarization P . T and $T + \delta T$ denote the temperatures of the N and S_R elements, respectively. (b) Total density of states v_{S_R} vs energy (E) in S_R showing the exchange-field-induced spin splitting. In the present case we set a finite $h = 0.3\Delta_R$ where Δ_R is the order parameter. (c) A superconducting quantum interference device (SQUID) containing a superconductor-normal metal-superconductor (S_LNS_L) proximity Josephson junction of length L . The loop is pierced by an external applied magnetic flux Φ which allows the DoS in the N region to be varied. ϕ is the quantum phase difference across the N wire. The proximity SQUID implements the phase-coherent element of the transistor. (d) Density of states v_N in the N wire vs energy E calculated for a few values of the applied magnetic flux. Φ_0 denotes the flux quantum. (e) Sketch of the resulting phase-coherent thermoelectric transistor obtained by joining the thermoelectric element in (a) with the S_LNS_L proximity SQUID shown in (c). In particular, the N wire is placed on top of the FI layer, and is therefore tunnel-coupled to S_R as in the scheme shown in panel (a). Under temperature bias, a thermovoltage V can develop across the transistor which can be finely tuned through the magnetic flux. S indicates the transistor Seebeck coefficient.

relations, its DoS can be expressed as^{6,7}

$$v_N(E, \Phi) = \left| \text{Re} \left[\frac{E + i\Gamma}{\sqrt{(E + i\Gamma)^2 - \Delta_L^2(T) \cos^2(\pi\Phi/\Phi_0)}} \right] \right|, \quad (3)$$

where Δ_L is the order parameter of the superconducting loop. Equation (3) explicitly shows that v_N can be modulated by the magnetic flux. As displayed in Fig. 1(d), the induced gap is fully open for vanishing flux whereas it closes for $\Phi = \Phi_0/2$. As a consequence, the N metal behaves as a phase-tunable superconductor.

Our phase-coherent thermoelectric transistor is sketched in Fig. 1(e). It combines both the proximity SQUID and the S_R spin-split superconductor. The S_R electrode is tunnel-coupled to the middle of the N wire through the FI layer. Therefore, the probability for electrons to tunnel between N and S_R depends on the sign of the spin. The device resembles the superconducting quantum interference proximity transistor (SQUIPT)⁸⁻¹² which has been well-studied in several experiments; the crucial structural difference in our device is that the thermoelectric transistor lies in the presence of the FI

layer.

The efficiency of the thermoelectric transistor can be finely tuned by the applied magnetic flux. To determine the ideal conditions for large thermoelectric efficiency we calculate the linear response transport coefficients. In other words, we calculate the charge (I) and heat (\dot{Q}) currents flowing through the structure when either a small voltage V or a small temperature difference δT is applied across the junction. At steady state these currents are expressed as follows:

$$\begin{pmatrix} I \\ \dot{Q} \end{pmatrix} = \begin{pmatrix} \sigma & \alpha \\ \alpha & \kappa T \end{pmatrix} \begin{pmatrix} V \\ \delta T/T \end{pmatrix}. \quad (4)$$

Here, α is the thermoelectric coefficient defined in Eq. (2) which has now become phase dependent through $v_N(E, \Phi)$. As well as the the electric (σ) and the thermal (κ) conduc-

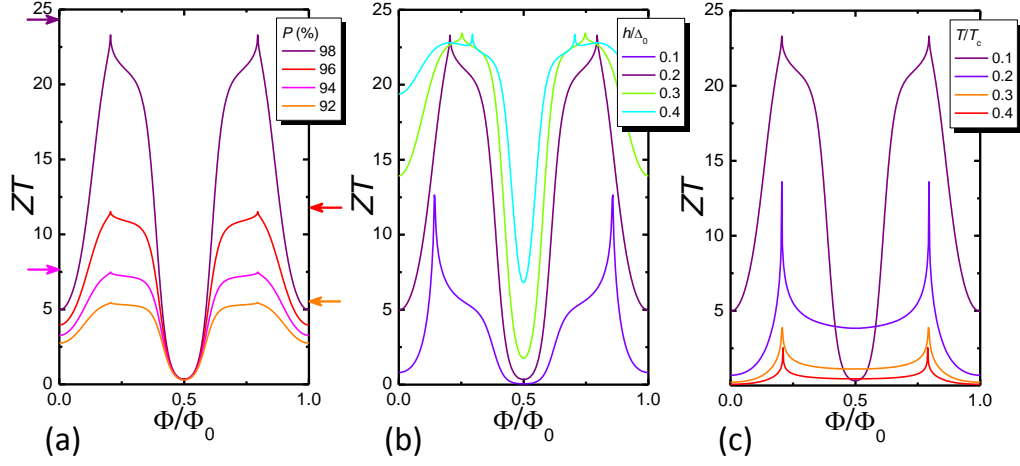


FIG. 2. Thermoelectric transistor figure of merit ZT . (a) Transistor thermoelectric figure of merit ZT vs magnetic flux Φ calculated for a few polarization values (P) of the FI layer at $h = 0.2\Delta_0$ and $T = 0.1T_c$. Colored arrows indicate the zero-temperature limit $ZT = P^2/(1 - P^2)$ for the given barrier polarizations. (b) ZT vs Φ calculated for some exchange field values at $T = 0.1T_c$ and $P = 98\%$. (c) ZT vs Φ calculated for a few temperatures T assuming $P = 98\%$ and $h = 0.2\Delta_0$. $T_c \approx \Delta_0/1.764k_B$ is the common critical temperature of both superconductors forming the thermoelectric device, and Δ_0 is the zero-temperature, zero-exchange field energy gap.

tances given by the expressions:⁴

$$\sigma(\Phi) = \frac{1}{R_T} \int_{-\infty}^{\infty} dE \frac{v_N(E, \Phi) \left[v_{S_{R\uparrow}}(E) + v_{S_{R\downarrow}}(E) \right]}{4k_B T \cosh^2\left(\frac{E}{2k_B T}\right)}, \quad (5a)$$

$$\kappa(\Phi) = \frac{1}{e^2 R_T} \int_{-\infty}^{\infty} dE \frac{E^2 v_N(E, \Phi) \left[v_{S_{R\uparrow}}(E) + v_{S_{R\downarrow}}(E) \right]}{4k_B T^2 \cosh^2\left(\frac{E}{2k_B T}\right)}. \quad (5b)$$

The thermoelectric efficiency of the transistor can be quantified by the usual dimensionless figure of merit ZT defined as

$$ZT = \frac{S^2 \sigma T}{\tilde{\kappa}}, \quad (6)$$

where $\tilde{\kappa} = \kappa - \alpha^2/\sigma T$ is the thermal conductance at zero current and $S = -\alpha/(\sigma T)$ the Seebeck coefficient that is a measure for the thermopower [see Fig. 1(e)]. We stress that there is no theoretical limit for ZT : if it approaches infinity the efficiency of the transistor would reach the Carnot limit. So far, only exceptionally-good thermoelectric bulk materials are able to provide values of ZT slightly larger than 1 [see Fig. 4(a)]. By contrast, our thermoelectric transistor can result in ZT values as large as several tens thanks to the fine tuning offered via the phase. This is displayed in Fig. 2 where the flux dependence of ZT as a function of different parameters is shown. In Fig. 2(a) the temperature and splitting field are fixed at moderate values, $0.1T_c$ and $0.2\Delta_0$, respectively.^{14,16–18} $T_c \approx (1.764k_B)^{-1}\Delta_0$ denotes the superconducting critical temperature, Δ_0 is the zero-temperature, zero-exchange field energy gap, and for clarity we assume that both S_L and S_R have the same Δ_0 value. Therefore, by tuning the flux through the loop the theoretical zero-temperature limit assuming no inelastic scattering processes for $ZT = P^2/(1 - P^2)$ (indicated

by colored arrows corresponding to each P value)⁴ can be approached without requiring ultra-low temperatures. It is also apparent that a high barrier polarization is crucial in order to achieve large values of ZT . Good candidates for the tunneling

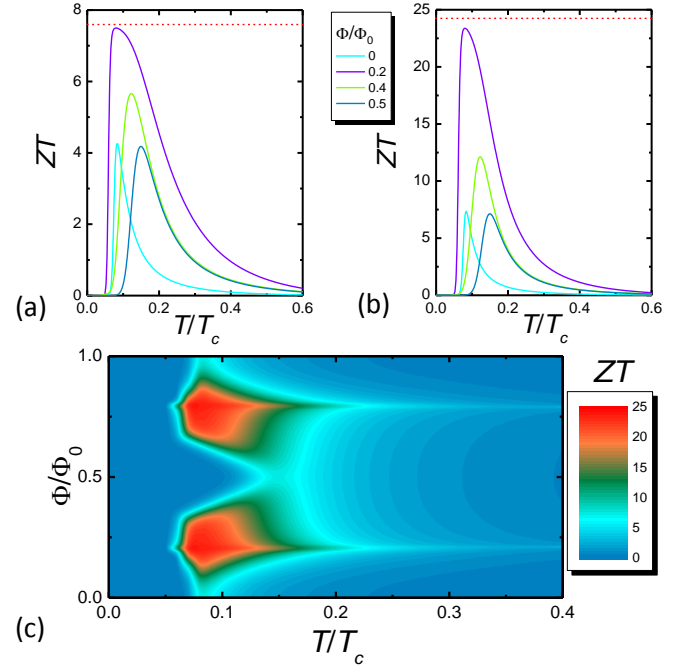


FIG. 3. Full temperature and magnetic flux behavior of the thermoelectric figure of merit. (a) Thermoelectric figure of merit ZT vs temperature T calculated for a few values of the applied flux Φ at $h = 0.2\Delta_0$ and $P = 94\%$. (b) The same as in panel (a) but calculated for $P = 98\%$. Red dashed lines in panels (a) and (b) indicate the zero-temperature limit for the above given barrier polarizations. (c) Color plot of ZT vs T and Φ calculated at $h = 0.2\Delta_0$ and for $P = 98\%$.

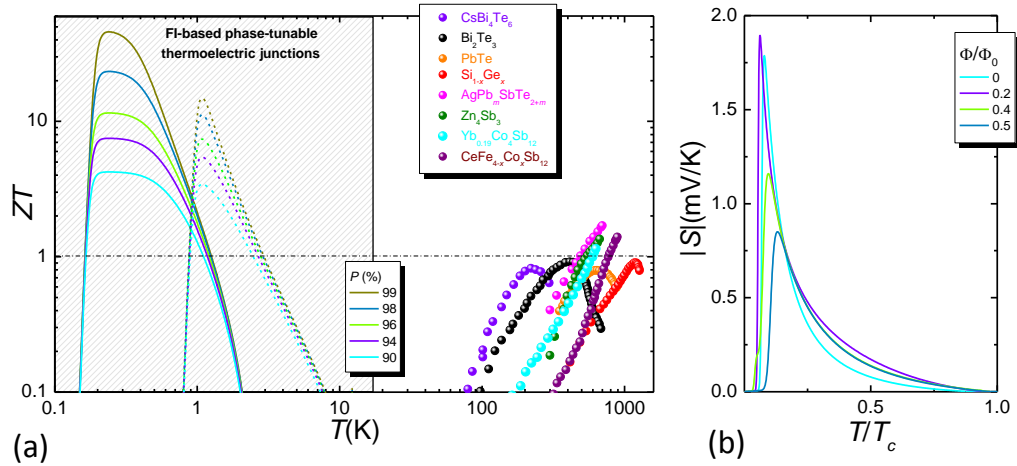


FIG. 4. Comparison of the transistor performance with state-of-the-art high- ZT materials and the achievable Seebeck coefficient. (a) Left side: Expected figure of merit ZT vs T for an EuS/Al-type (solid lines) and GdN/NbN-type (dashed lines) phase-coherent thermoelectric transistors calculated for selected values of the barrier polarization. We assumed $T_c = 3\text{K}$ and $h = 0.2\Delta_0$ for the former structure whereas for the latter we set $T_c = 14\text{K}$ and $h = 0.1\Delta_0$. Furthermore, for both of them we set $\Phi = 0.2\Phi_0$. Right side: Figure of merit ZT vs temperature possessed by several state-of-the-art commercial bulk thermoelectric materials. Dash-dotted line indicates $ZT = 1$. (b) Absolute value of the Seebeck coefficient (S) achievable in the phase-coherent thermoelectric transistor vs T calculated for a few selected values of the applied magnetic flux at $h = 0.2\Delta_0$ and $P = 98\%$. Data shown in panel (a) are taken from Ref.²⁷.

barriers are europium chalcogenides (EuO and EuS) for which values of P ranging from 80 up to almost 100% have been reported.^{13–16,18–21} Also very high spin-filtering has been reported in GdN barriers^{22–24} with polarizations as large as 97% at 15 K (even larger values are expected as T decreases).

In Fig. 2(b) P is set to 98%, $T = 0.1T_c$ and ZT for different values of the induced Zeeman field h is plotted showing an interesting non-monotonic behavior. h cannot be externally tuned but can be partially controlled during growth of the FI/S_R interface since it depends on the quality of the contact. Values from 0.1 meV up to few meV for the Zeeman splitting have been reported.^{16,21,25,26}

We emphasize that the amplitude of the thermoelectric effect also depends on the length of the N wire. We assumed that L is smaller than the superconducting coherence length [see Eq. (3)] or meaning $\Delta_0 < \epsilon_{Th}$, where $\epsilon_{Th} = \hbar D/L^2$ is the Thouless energy and D the diffusion coefficient of the N wire. Although these two energies in the existing experiments on SQUIPTs are of same order^{11,12}, the observed modulation of the induced gap by the magnetic flux can be well described with Eq. (3)¹². Instead of the N bridge one can use a short constriction made with the same material of the loop. In such a case one avoids the mismatch of the Fermi velocities at the interfaces, meaning the proximity effect between the bulky part of the loop and the constriction is increased.

Figure 2(c) shows the flux dependency of ZT for different values of the temperature, at $P = 98\%$ and $h = 0.2\Delta_0$. It is clear that the efficiency of the transistor decreases by increasing the temperature towards T_c .

Figures 3(a) and 3(b) show the temperature dependence of ZT for different magnetic fluxes. ZT reaches a maximum at a finite T that corresponds to the temperature for which the difference between the gap induced in N and the gap in the S_R electrode matches the value of the exchange field, i.e., when

the coherent peaks in the DoS at the edges of the gaps [see Figs. 1(b) and 1(d)] coincide. The red dashed lines in Figs. 3(a) and 3(b) show the upper theoretical value of ZT at zero temperature⁴. Our device, however, allows to approach this maximum value at finite T by tuning the magnetic flux. The full dependence of ZT on both T and Φ , for $P = 98\%$ and $h = 0.2\Delta_0$ is shown by the color plot in Fig. 3(c). For $T \approx 0.1T_c$ and $\Phi \approx 0.25\Phi_0$ or $\Phi \approx 0.75\Phi_0$ the figure of merit can reach values close to $P^2/(1 - P^2) \approx 25$.

To place our device in the context of thermoelectrics we show in Fig. 4(a) the state-of-the-art bulk materials with the highest ZT values. One of the most widely used material is Bi_2Te_3 ,^{27,28} which at room temperature shows a ZT close to 1. All other materials show their highest values of ZT at high temperatures. By contrast, our transistor operates at low temperatures where it can reach values of ZT which are larger by more than an order of magnitude. An appropriate candidate is EuO combined with superconducting Al where we expect a ZT of $\sim 30 - 40$ for realistic values of the spin-filter efficiency.^{15,19} Other suitable Eu chalcogenides include EuS or EuSe. In the latter case P and h can be tuned by an external magnetic field.¹⁸ An alternative to the chalcogenides is to use GdN with superconducting NbN.^{22,24} Its advantage is the higher critical temperature of NbN of $\simeq 15\text{K}$. As for the normal metal bridge, it is important to achieve good electric contact with the S_R loop in order to develop a sizeable and tunable proximity gap. If, for instance, one uses Al as superconductor for the ring, suitable candidates for the N wire are copper (Cu)^{8,9,11,12} or silver (Ag)²⁹.

The temperature-voltage conversion capability of the thermoelectric transistor can be quantified by the Seebeck coefficient S : its temperature dependence is shown in Fig. 4(b) for selected values of the applied magnetic flux. Here we set $P = 98\%$ and $h = 0.2\Delta_0$. The transistor is extremely sensi-

tive at low temperatures, and provides a sharp response even to tiny temperature gradients. In particular, Seebeck coefficients as large as a few mV/K can be achieved under optimal flux tuning conditions, which have to be compared to coefficients as large as a few hundreds of $\mu\text{V/K}$ obtained in the abovementioned high-performance thermoelectric materials. These sizeable values of S make our phase-coherent thermoelectric transistor an ideal candidate for the implementation of cryogenic power generators or ultrasensitive low-temperature general purpose thermometry as well as, for radiation sensors where heating of one of the superconductors forming the junction is achieved due to a coupling with radiation.

The work of F.G. has been partially funded by the European Research Council under the European Union's Seventh Framework Programme (FP7/2007-2013)/ERC grant agreement No. 615187-COMANCHE, and by the Marie Curie Initial Training Action (ITN) Q-NET 264034. J.W.A.R. acknowledges funding from the Royal Society ("Superconducting Spintronics"). J.W.A.R. and F.S.B. jointly acknowledge funding from the Leverhulme Trust through an International Network Grant (grant IN-2013-033). J.S.M acknowledges funding from the National Science Foundation ((grant DMR 1207469) and the Office of Naval Research (grant N00014-13-1-0301). The work of F.S.B. has been supported by the Spanish Ministry of Economy and Competitiveness under Project No. FIS2011-28851-C02-02.

¹N. W. Ashcroft and D. N. Mermin, *Solid State Physics* (Saunders College, Philadelphia, 1976).

²G. D. Mahan, *J. Appl. Phys.* **65**, 1578 (1989).

³P. Machon, M. Eschrig, and W. Belzig, *Phys. Rev. Lett.* **110**, 047002 (2013).

⁴A. Ozaeta, P. Virtanen, F. Bergeret, and T. T. Heikkilä, *Phys. Rev. Lett.* **112**, 057001 (2014).

⁵P. Machon, M. Eschrig, and W. Belzig, arXiv: 1402.7373 (2014).

⁶A. Golubov and M. Y. Kupriyanov, *Zh. Eksp. Teor. Fiz* **96**, 1420 (1989).

⁷T. T. Heikkilä, J. Särkkä, and F. K. Wilhelm, *Phys. Rev. B* **66**, 184513 (2002).

⁸F. Giazotto, J. T. Peltonen, M. Meschke, and J. P. Pekola, *Nat. Phys.* **6**, 254 (2010).

⁹M. Meschke, J. T. Peltonen, J. P. Pekola, and F. Giazotto, *Phys. Rev. B* **84**, 214514 (2011).

¹⁰F. Giazotto and F. Taddei, *Phys. Rev. B* **84**, 214502 (2011).

¹¹R. N. Jabdaraghi, M. Meschke, and J. Pekola, *Appl. Phys. Lett.* **104**, 082601 (2014).

¹²A. Ronzani, C. Altimiras, and F. Giazotto, arXiv:1404.4206.

¹³J. Moodera, X. Hao, G. Gibson, and R. Meservey, *Phys. Rev. Lett.* **61**, 637 (1988).

¹⁴X. Hao, J. Moodera, and R. Meservey, *Phys. Rev. B* **42**, 8235 (1990).

¹⁵T. S. Santos and J. S. Moodera, *Phys. Rev. B* **69**, 241203 (2004).

¹⁶J. S. Moodera, T. S. Santos, and T. Nagahama, *Jour. of Phys.: Cond. Matt.* **19**, 165202 (2007).

¹⁷R. Meservey and P. M. Tedrow, *Phys. Rep.* **238**, 173 (1994).

¹⁸J. S. Moodera, R. Meservey, and X. Hao, *Phys. Rev. Lett.* **70**, 853 (1993).

¹⁹T. S. Santos, J. S. Moodera, K. V. Raman, E. Negusse, J. Holroyd, J. Dvorak, M. Liberati, Y. U. Idzerda, and E. Arenholz, *Phys. Rev. Lett.* **101**, 147201 (2008).

²⁰G.-X. Miao and J. S. Moodera, *App. Phys. Lett.* **94**, 182504 (2009).

²¹B. Li, N. Roschewsky, B. A. Assaf, M. Eich, M. Epstein-Martin, D. Heiman, M. Mnzenberg, and J. S. Moodera, *Phys. Rev. Lett.* **110**, 097001 (2013).

²²K. Senapati, M. G. Blamire, and Z. H. Barber, *Nat. Mat.* **10**, 1 (2011).

²³A. Pal, Z. Barber, J. Robinson, and M. Blamire, *Adv. Mat.* **25**, 5581 (2013).

²⁴A. Pal, K. Senapati, Z. Barber, and M. Blamire, *Nat. Comm.* **5** (2014).

²⁵P. M. Tedrow, J. E. Tkaczyk, and A. Kumar, *Phys. Rev. Lett.* **29**, 1651 (1986).

²⁶X. Hao, J.S. Moodera, and R. Meservey, *Phys. Rev. Lett.* **67**, 1342 (1991).

²⁷T. M. Tritt and M. Subramanian, *MRS Bulletin* **31**, 188 (2006).

²⁸G. J. Snyder and E. S. Toberer, *Nat. Mat.* **7**, 105 (2008).

²⁹H. Le Sueur, P. Joyez, H. Pothier, C. Urbina, and D. Esteve, *Phys. Rev. Lett.* **100**, 197002 (2008).